Difference Frequency Generation by Quasi-Phase Matching in Periodically Intermixed Semiconductor Superlattice Waveguides

Sean J. Wagner, *Member, IEEE*, Barry M. Holmes, *Member, IEEE*, Usman Younis, Iliya Sigal, Amr S. Helmy, *Senior Member, IEEE*, J. Stewart Aitchison, *Senior Member, IEEE*, and David C. Hutchings, *Senior Member, IEEE*

***Abstract*—Wavelength conversion by difference frequency generation is demonstrated in domain-disordered quasi-phase matched waveguides. The waveguide structure consisted of a GaAs/AlGaAs superlattice core that was periodically intermixed by ion-implantation. For quasi-phase matching periods of 3.0–3.8 μm, degeneracy pump wavelengths were found by second-harmonic generation experiments for fundamental wavelengths between 1520–1620 nm in both type-I and type-II configurations. In the difference frequency generation experiments, output powers up to 8.7 nW were generated for the type-I phase matching interaction, and 1.9 nW for the type-II interaction. The conversion bandwidth was measured to be over 100 nm covering the C, L, and U optical communications bands, which agrees with predictions.**

***Index Terms*—nonlinear optics, difference frequency generation, semiconductor superlattice, quantum-well intermixing**

I. Introduction

SECOND-ORDER nonlinear optical frequency conversion processes are widely used for generating new optical wavelengths, particularly in regions of the electromagnetic spectrum where there are no suitable laser sources. Frequency downconversion also has applications for all-optical channel conversion in high-speed telecommunications systems. As these processes do not require the optical frequency to be coincident with a material resonance, wide wavelength tunability is normally possible. Most nonlinear optical source systems based on parametric wavelength conversion to date generally use bulk nonlinear crystals, such as periodically-poled $LiNbO_3$ (PPLN), KTP or BBO. These tend to be based on discrete components that require assembly and are hence relatively large and expensive. Therefore, there is a requirement for making such systems more compact and lower power, and for employing integration techniques to replace manual assembly. As a first step, nonlinear waveguides extend the length of the optical interaction beyond what can be normally achieved with focused beams in a bulk crystal. Hence, PPLN waveguides are becoming increasingly deployed for difference frequency and parametric generation [1]–[3].

The GaAs/AlGaAs semiconductor material system has been of interest as an alternative platform for parametric conversion devices. Compound semiconductors exhibit large nonlinear optical susceptibilities. Lithography and fabrication technologies for AlGaAs are mature and well established, leading to low manufacturing costs, high yields, and mass production. The typically large value for the refractive index and the ability to form waveguides by etching facilitates a much reduced mode cross-section in comparison to ion exchange waveguides in ferroelectrics. Hence, the size and power requirements for a parametric conversion device can potentially be reduced substantially. Furthermore, the transparency range of AlGaAs extends to 17 μm, which is further into the mid-infrared than typical ferroelectric crystals. This permits generation of an extended range of mid-IR wavelengths that are of interest for spectroscopy and optical sensing. GaAs/AlGaAs is a direct band gap semiconductor capable of efficiently emitting light and hence there is the potential for monolithically integrating pump laser sources directly on-chip. The power requirements can be reduced further with the incorporation of the nonlinear conversion element within the laser cavity itself.

Despite these advantages, phase matching the nonlinear conversion process remains a challenge as AlGaAs is isotropic and lacks a natural birefringence. Hence, artificial structures need to be implemented in order to meet the phase matching condition. There are several methods for achieving phase matching in III-V semiconductors [4] and thus far, difference frequency generation (DFG) has been demonstrated in form-birefringent GaAs/Al_yO_x waveguides [5], [6], wafer-bonded domain-reversal quasi-phase matching (QPM) waveguides [7], orientation-patterned GaAs QPM waveguides [8], and modal phase matching Bragg reflection waveguides [9]. These platforms generally have a number of limitations, particularly where the monolithic integration of active optical devices such as lasers for pumping is considered, including the use of complex fabrication processes, inherently high propagation losses, incompatibility of the wafer growth process with doped heterostructures, and higher-order modal requirements.

Manuscript received ***; Revised ***; Accepted ***; Date of current version ***.

This work was supported by grants from the U.K. Engineering and Physical Sciences Research Council, and the Natural Sciences and Engineering Research Council of Canada. U. Younis' work was supported by NUST SEECS. S. J. Wagner's work was supported by an NSERC Postgraduate Scholarship.

S. J. Wagner, I. Sigal, A. S. Helmy, and J. S. Aitchison are with the Edward S. Rogers Sr. Department of Electrical and Computer Engineering, University of Toronto, 10 King's College Road, Toronto, Ontario, M5S 3G4, Canada (E-mail: sean.wagner@utoronto.ca)

B. M. Holmes, U. Younis, and D. C. Hutchings are with the School of Engineering, University of Glasgow, Glasgow, G12 8QQ, Scotland, UK

Color versions of one or more of the figures in this paper are available online at http://ieeexplore.ieee.org.

Digital Object Identifier ***

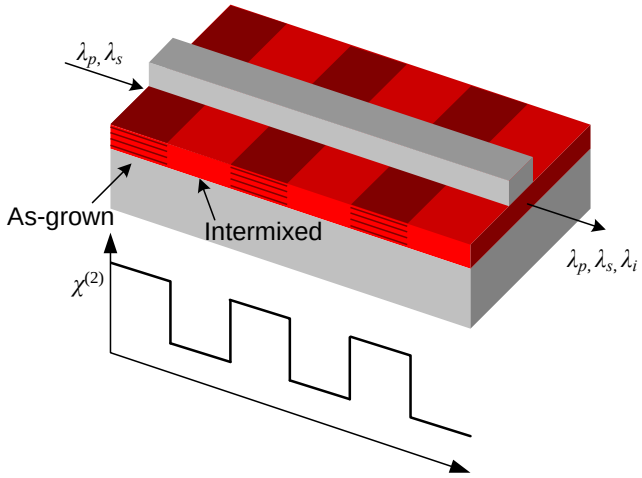

Fig. 1: Schematic of a domain-disordered quasi-phase matching waveguide. The superlattice core layer is patterned by quantum-well intermixing such that a grating with high (as-grown) and low (intermixed) $\chi^{(2)}$ is formed to mediate the difference frequency generation process such that the idler wavelength (λ_i) is efficiently generated by the pump (λ_p) and signal (λ_s) wavelengths.

We have been investigating the use of domain-disordered QPM (DD-QPM) structures in GaAs/AlGaAs superlattices [10]. In this method, depicted in Figure 1, a waveguide with a superlattice core is patterned by quantum-well intermixing (QWI) [11] to periodically suppress the second-order nonlinear susceptibility $\chi^{(2)}$. An advantage of using DD-QPM and a GaAs/AlGaAs superlattice platform is the potential to integrate the frequency conversion device with on-chip pump lasers. Recently, we demonstrated pump lasers emitting at around 800 nm, and wavelength multiplexing couplers using a superlattice waveguide structure [12]. Theoretical calculations from the superlattice electronic band structure have predicted that a large modulation in $\chi^{(2)}$ of up to 100 pm/V can be obtained using this approach [13]. Using DD-QPM waveguides, we have demonstrated continuous-wave second-harmonic generation (SHG) [14] and type-II phase matched SHG [15]. In this paper, we report on difference frequency generation with GaAs/AlGaAs superlattice-core domain-disordered quasi-phase matching waveguides. We show by calculations and experiments that the conversion bandwidth of such structures extends over 100 nm.

II. Theory

In order to obtain an indication of the form of the tuning curves for DFG and parametric generation, we make use of the refractive index measurements reported in [16]. In this paper, Bragg coupling measurements were performed for both TE- and TM-polarised modes in a slab waveguide containing a 600 nm 14:14 monolayer GaAs/AlAs superlattice core both as-grown and after QWI at wavelengths centered around 830 nm and 1520 nm. The QWI technique used in this paper was the sputtered silica method [17]. The QPM average refractive index is taken to be the simple average of the as-grown and QWI values, which are themselves obtained by quadratic fits to the measured data in each of the wavelength bands.

The phase-matching criterion for first-order QPM is given by

$$\frac{n_p}{\lambda_p} - \frac{n_s}{\lambda_s} - \frac{n_i}{\lambda_i} = \frac{1}{\Lambda} \tag{1}$$

where the subscripts p, s, and i indicate the pump, signal, and idler waves, respectively, and Λ is the QPM grating period. The wavelengths are constrained by energy conservation such that

$$\frac{1}{\lambda_p} = \frac{1}{\lambda_s} + \frac{1}{\lambda_i}. \tag{2}$$

In the type-I configuration the relevant tensor component is $\chi^{(2)}_{zxy}$ with the shorter wavelength component (pump) being TM-polarised and the longer wavelength components (signal and idler) both TE-polarised. Figure 2(a) shows the calculated tuning curves for a three-wave interaction in the type-I configuration for the indicated QPM grating periods. Figure 2(b) shows the detail of the tuning curve around the degeneracy point (corresponding to second harmonic generation) for a grating period $\Lambda = 3.8$ μm, with the short-dashed lines indicating where the phase mis-match reaches $\Delta kL = \pm\pi$ (first zero for the sinc^2 conversion) for a 1 mm long waveguide. Therefore, even up to a ∼150 nm separation of the signal and idler wavelengths will still lie within the main lobe of the conversion efficiency using a pump wavelength corresponding to the degeneracy point.

In the type-II configuration the relevant tensor component is $\chi^{(2)}_{xyz}$ with the shorter wavelength component (pump) being TE-polarised and of the longer wavelength components (signal and idler), one is TE-polarised and the other TM-polarised. The type-II configuration is appropriate for the monolithic integration of a pump source, which normally emits only TE-polarised light. Figure 3 shows the calculated tuning curves for a three-wave interaction in the type-II configuration for the QPM grating periods shown. Figure 3(b) shows the detail of the tuning curve around the degeneracy point (corresponding to type-II second harmonic generation) for a grating period $\Lambda = 3.4$ μm. Again, the short-dashed lines indicating where the phase mis-match reaches $\Delta kL = \pm\pi$ for a 1 mm long waveguide. The signal and idler are orthogonally polarised in this configuration so the tuning curves are not coincident, except at the degeneracy point. Furthermore, the degeneracy point does not necessarily correspond to the longest pump wavelength which can support a three-wave interaction. Starting from the degeneracy point and keeping the pump wavelength fixed, it is expected that the TE-component can be tuned up to ∼60 nm below the degeneracy point, or by up to a value much larger than the ∼100 nm range shown in the figure above the degeneracy point, and still lie within the main lobe of the conversion.

III. Sample Fabrication

The waveguide structure used for DFG experiments was the same as that in [14]. It consisted of a 600 nm thick core layer of 14:14 monolayer GaAs/$Al_{0.85}Ga_{0.15}As$ superlattice. On either side were 300 nm thick buffer layers of $Al_{0.56}Ga_{0.44}As$

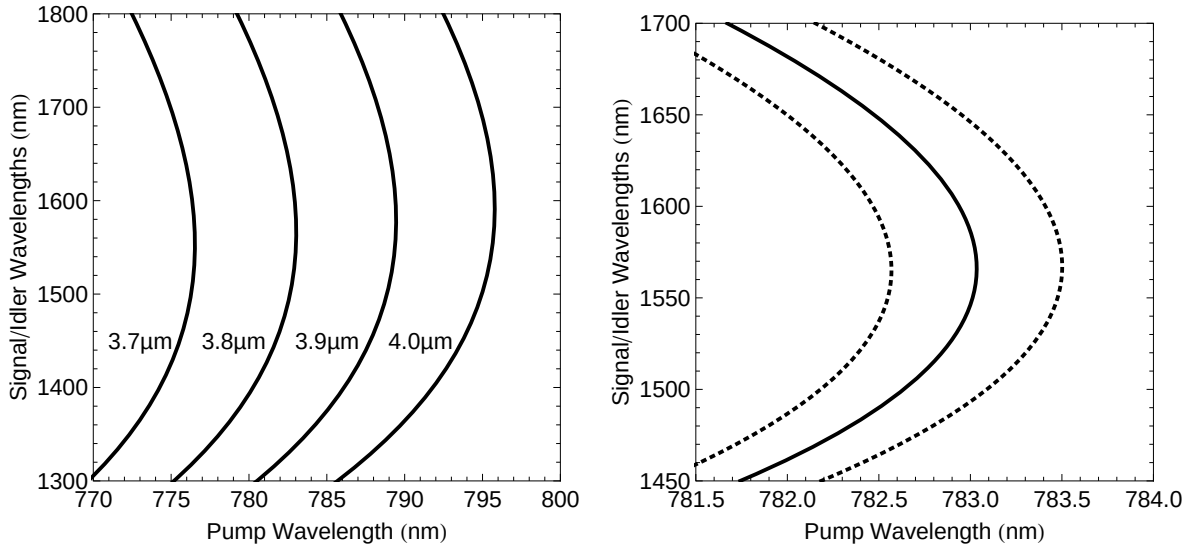

Fig. 2: Calculated tuning curves for a three-wave interaction in a type-I configuration (a) for the QPM grating periods Λ =3.7–4.0 μm. (b) detail around the degeneracy point for Λ =3.8 μm. The short-dashed lines in (b) show the completely out-of-phase wavelength combinations for a 1 mm waveguide length.

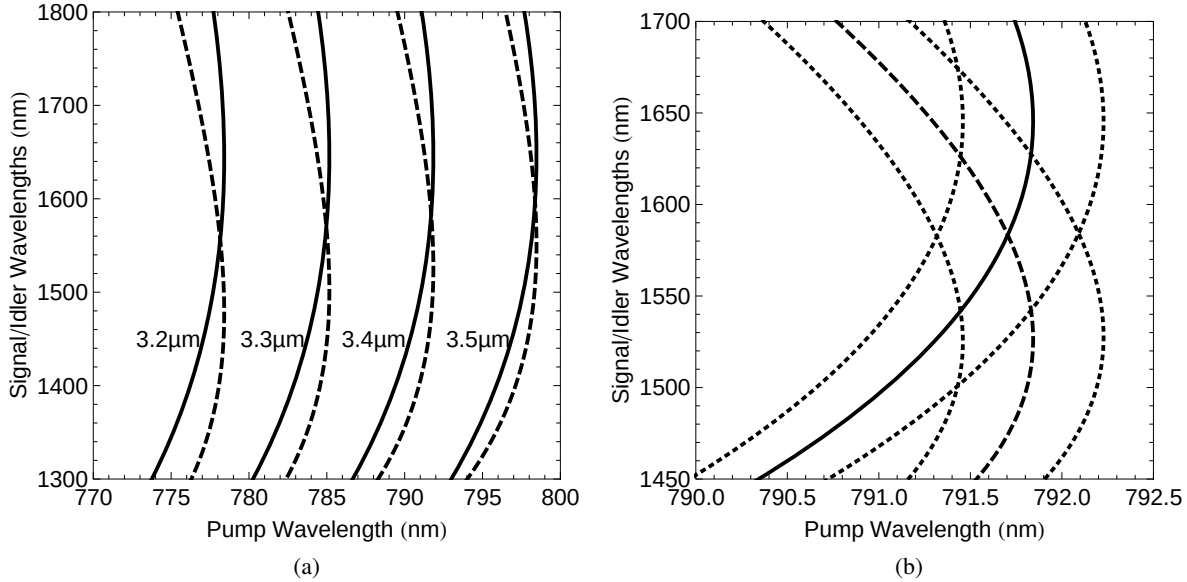

Fig. 3: Calculated tuning curves for a three-wave interaction in a type-II configuration, with the solid and dashed curves corresponding to the TE and TM-polarised components respectively, (a) for the QPM grating periods Λ =3.2–3.5 μm. (b) detail around the degeneracy point for Λ =3.4 μm. The short-dashed lines in (b) show the completely out-of-phase wavelength combinations for a 1 mm waveguide length.

and 800 nm thick $Al_{0.60}Ga_{0.40}As$ cladding layers. A 1.0 μm thick base layer of $Al_{0.85}Ga_{0.15}As$ was added below the lower cladding layer to isolate the optical modes from the substrate. All layers were grown on a semi-insulating GaAs substrate by molecular beam epitaxy.

DD-QPM gratings were formed by patterned QWI of the superlattice using ion implantation. A mask was formed by first using electron-beam lithography to write gratings of a range of periods in poly(methyl methacrylate) (PMMA) with a drawn duty cycle of 40%. A 2.3 μm thick Au implantation mask was deposited in the PMMA gaps by electroplating and the PMMA subsequently removed. Inspection of the mask showed that the proportion of open areas was slightly reduced from the nominal 40% value as written in PMMA. Ion implantation was carried out with 4.0 MeV As^{2+} ions at a dosage of 2.0×10^{13} cm^{-2} followed by rapid thermal annealing (RTA) at 775°C for 60 s. Lateral ion straggle results in implantation over a larger area than defined by the mask openings, and QWI is mediated by subsequent diffusion of the point defects under RTA. Thus, the variation in $\chi^{(2)}$

with distance is not necessarily simply represented by the drawn grating duty cycle. Photoluminescence measurements at 77 K showed a band gap energy blue-shift of 76 nm in the intermixed regions of the sample.

Ridge waveguides 3.0 μm wide and 1.3 μm deep were fabricated by reactive ion etching and the final sample was cleaved to a length of 1 mm. Linear losses in these waveguides around 1550 nm measured by the Fabry-Perot method averaged 1.8 cm^{-1} in the TE polarisation and 3.7 cm^{-1} in the TM polarisation. Losses around 790 nm were estimated as 13 cm^{-1} for the TM polarisation and 24 cm^{-1} for the TE polarisation using a combination of Fabry-Perot and transmission measurements.

IV. Optical Measurements

SHG measurements were first carried out to identify the degeneracy wavelengths for DFG. Measurements were carried out using the ∼2 ps pulsed setup described in [15], which consisted of an optical parametric oscillator pumped by a modelocked Ti:sapphire laser. The phase matching wavelengths at which SHG efficiency was highest were measured for various QPM grating periods and are shown in Figure 4. The dashed lines indicate the phase-matching wavelengths based on the refractive index measurements reported in [16]. Note that there are significant differences between the samples used in the refractive index measurements from which the expected tuning curves were obtained, and those in the current frequency mixing experiments: (1) the wafer composition is different with the superlattice AlAs barriers replaced with $Al_{0.85}Ga_{0.15}As$; (2) the QWI technique was replaced with a high-resolution ion-implantation induced method; (3) slab waveguides were replaced with rib waveguides providing lateral optical confinement. Despite the sample differences, the predicted and measured variation of the phase-matching wavelength as a function of grating period have a similar form.

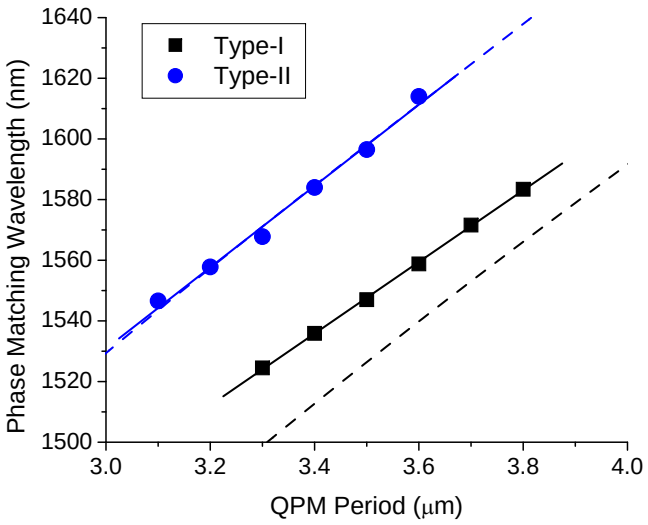

Fig. 4: Phase matching wavelengths for type-I and type-II SHG with several different QPM periods. Solid lines show the best linear fit to the measured data points. Dashed lines show the predicted phase matching wavelengths from the refractive index measurements in [16].

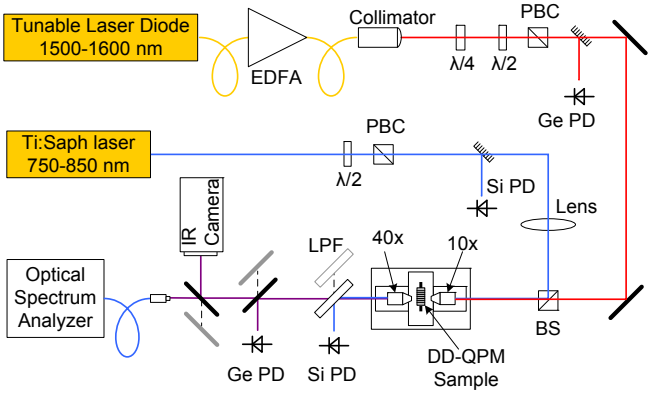

Fig. 5: Schematic of the DFG experiment. The signal beam from the tunable diode laser and the pump beam from the Ti:sapphire laser are combined in the beam splitter (BS) and launched into the waveguide sample. On the output side of the sample, the pump beam is separated from the transmitted signal and generated idler beams by a low-pass filter (LPF).

Difference frequency generation experiments were carried out using the setup depicted in Figure 5. The Ti:sapphire laser was used as the pump wavelength source in continuous wave mode. The signal wavelength source was a tunable continuous wave C-Band laser followed by an erbium-doped fiber amplifier (EDFA). Signal and pump beams were combined by a beam splitter and coupled into the waveguide using a 10× objective lens. To compensate for the difference in the focusing length between the pump and signal beams in this objective, a 300 mm focal length spherical lens was inserted into the pump beam path before the beam splitter. Output light from the waveguide was collected by a 40× objective lens. The output pump and signal wavelengths were split using a long-pass filter and focused onto separate photodetectors for power measurements. To identify the generated idler wavelength, the output beam was directed to a fiber-coupled optical spectrum analyzer (OSA).

We investigated type-I phase matched DFG by setting the signal to the TE polarisation and the pump to the TM polarisation. For the 3.8 μm QPM period, the pump wavelength was initially set to 791.7 nm for the degeneracy point as prescribed by the SHG measurement. The input signal power at the waveguide facet was 252 mW and input pump power was 45 mW. Transmission through the waveguide was observed to be 12.3% for the signal and 10% for the pump. The signal wavelength was adjusted over a few 10s of picometers to coincide with a Fabry-Perot resonance of the waveguide such that transmission and internal signal power were maximized. The signal wavelength range was constrained to less than 1560 nm such that the idler wavelength would be generated at wavelengths above 1600 nm where the amplified spontaneous emission (ASE) of the EDFA rolls off. The pump wavelength was slowly increased by up to 0.5 nm from its initial value to the point where the observed idler power peaked on the OSA, satisfying the phase-matching condition. This is within the accuracy for wavelength measurements using the OSA, but with

continuous-wave inputs for both the pump and signal, there is likely to be significant heating of the sample. Hence the increase of the pump wavelength to maintain phase-matching could be in compensation for the thermo-optic effects causing a shift in the tuning curve, which was observed previously for SHG [14]. For a 1550.1 nm signal wavelength, the idler wavelength was found at 1620.7 nm. The output idler was found to be TE polarised, which is consistent with the type-I phase matching configuration.

To obtain the output idler power value, it was necessary to account for the coupling ratio into the input fiber of the OSA. This was done by comparing the signal wavelength peak power on the OSA with the power measured on the photodetector to derive a scaling factor. The idler power was then determined by multiplying the idler peak in the output spectrum measured on the OSA by this factor. After subtracting the ASE power and accounting for the output facet reflectivity, the internal output idler power was calculated to be 8.6 nW. The internal input signal power and pump power were calculated as 48.7 mW and 24.4 mW respectively after accounting for the facet reflectivity and linear losses. Thus, the signal-to-idler conversion efficiency was –67.5 dB. The normalized conversion efficiency for DFG is defined as

$$\eta = \frac{P_i}{P_s P_p L^2} \tag{3}$$

where P_i, P_s, and P_p are the powers of the idler, signal, and pump, respectively, and L is the waveguide length. Using this definition, the efficiency was calculated as 0.072 %W^{-1}cm^{-2}. The linear loss can be taken into account to give the ratio of the measured conversion efficiency and the efficiency in the lossless case (η_0) by the equation

$$\frac{\eta}{\eta_0} = \exp[-\tfrac{1}{2}(\alpha_s + \alpha_i + \alpha_p)L]\frac{\sinh^2(\tfrac{1}{2}\Delta\alpha L)}{(\tfrac{1}{2}\Delta\alpha L)^2} \tag{4}$$

where α_i, α_s, and α_p are the loss coefficients of the idler, signal, and pump, respectively, and $\Delta\alpha = \frac{1}{2}(\alpha_s + \alpha_p - \alpha_i)$. Using this, the lossless conversion efficiency was calculated as 0.19 %W^{-1}cm^{-2}.

The signal wavelength was scanned from 1535 to 1555 nm to test tuning of the idler. Figure 6 shows the recorded output spectra from the QPM waveguide for several signal wavelengths. The conversion efficiency was relatively uniform across this range, with the output idler power varying by less than 5 dB. Considering that the gain is expected to be relatively flat over this region, the conversion band likely extends from at least 1535 to 1637 nm without significant variation in the required pump wavelength. This represents a conversion bandwidth of over 100 nm, which spans the C, L, and U optical communications bands. The bandwidth may extend farther, however, limitations on the source wavelengths available and the detection ranges preclude more extensive testing.

Wavelength conversion by type-I DFG was also observed in a waveguide with a QPM period of 3.7 μm. The pump wavelength was initially set to 786 nm. While the idler peaks were clearly visible on the OSA, the peaks were at least 3 dB lower than in the 3.8 μm period waveguide. As a result, idler powers were only 2 dB above the ASE noise. This was

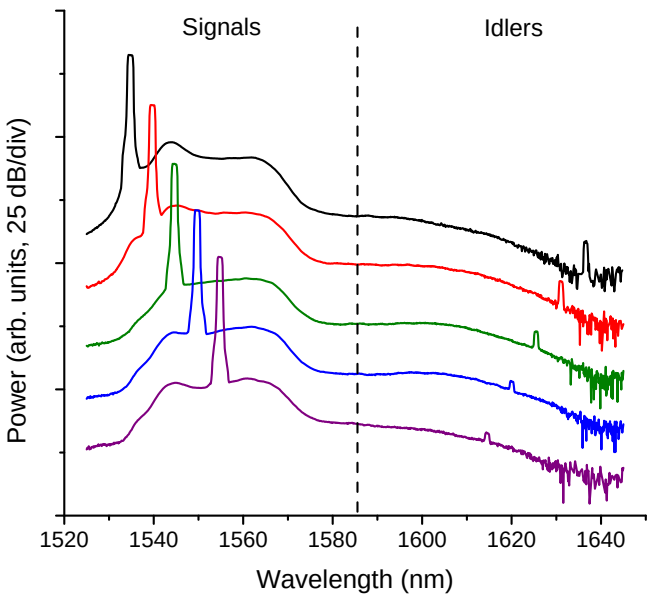

Fig. 6: Output spectra for type-I phase matching in a QPM waveguide for several signal wavelengths. The QPM period was 3.8 μm. The pump wavelength was initially set to 791.7 nm and adjusted by no more than ∼0.5 nm to maximize idler generation. Signal wavelengths are shown on the left and the generated idler wavelengths are shown on the right.

expected since this waveguide's degeneracy point corresponds to a shorter pump wavelength, and therefore it experiences more band tail absorption. As a result, the effective conversion efficiency was lower in this shorter QPM period.

Type-II phase-matched DFG was observed in a waveguide with a 3.4 μm QPM period. The pump was set to the TE polarisation and to the type-II degeneracy wavelength for this waveguide, which was near 792.9 nm. Figure 7 shows the recorded output spectrum for two different polarisation setups: a) TE signal, TM idler, and b) TM signal, TE idler. In both cases, the polarisation of the idler was confirmed by inserting a polariser just before coupling the light into the fiber attached to the OSA input. The signal wavelength still shows up in the spectral plots since the polariser only rejects about 20 dB of the orthogonal polarisation. The polariser also had the effect of reducing the noise in the spectral measurements by rejecting the orthogonally polarised contribution to the ASE noise present in the input beam, consequently increasing the contrast of the generated idler. The measured data from the OSA also shows the high-order diffraction from the pump wavelength, which is aliased to 1586 nm. The presence of the pump in the spectrum did not affect the measurement and provides a useful reference to the degeneracy wavelength.

Using the scaling factor method as outlined previously, the output idler power was calculated to be 1.9 nW at the exit facet of the waveguide for the TE signal, TM idler case. This is four times lower than in the type-I measurements, which is commensurate with similar trends observed in SHG experiments [15]. The internal input pump power was 31.3 mW, and the internal input signal power was 51.7 mW. Signal-to-idler conversion efficiency was –74.3 dB. From this, the

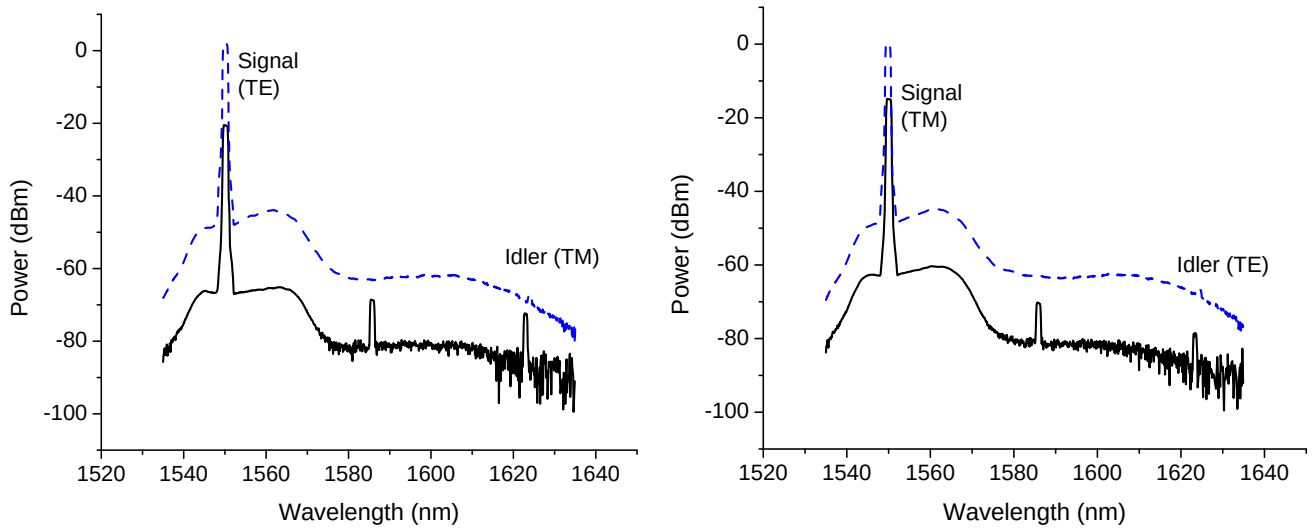

(a) (b)

Fig. 7: Output spectrum from a QPM waveguide under the type-II phase matching scheme. The QPM period was 3.4 μm, and the pump wavelength was initially set to 792.9 nm. The signal polarisation was set to (a) TE and (b) TM. The black (solid) lines show the spectrum with the idler polarisation isolated. The blue (dotted) line shows the measured spectrum without the polariser.

type-II normalized conversion efficiency was calculated as 0.012 $\%\mathrm{W}^{-1}\mathrm{cm}^{-2}$, which is six times lower than in the type-I case. The larger pump optical loss in the TE polarisation used for type-II phase matching is likely to significantly reduce the effective length of the nonlinear interaction and prove detrimental to the overall conversion efficiency. When accounting for the linear losses, the deduced lossless conversion efficiency becomes 0.044 $\%\mathrm{W}^{-1}\mathrm{cm}^{-2}$, which is still over four times lower than the type-I interaction.

V. Conclusions

In summary, difference frequency generation was demonstrated in GaAs/AlGaAs DD-QPM waveguides formed by periodic intermixing. Nearly 9 nW of idler power was generated for type-I phase matching, while type-II phase matching produced less than one fourth as much for similar signal and pump wavelengths. Tuning of the signal wavelength demonstrated conversion over 20 nm from the C-band to idler wavelengths in the L- and U-bands and showed that the total conversion bandwidth spans at least 100 nm without significant adjustment of the pump wavelength.

Acknowledgements

The authors thank the University of Surrey Ion Beam Centre for carrying out the ion implantation. We also acknowledge the valuable contributions by the technical support staff of the James Watt Nanofabrication Centre at the University of Glasgow.

References

[1] C. Q. Xu, H. Okayama, and M. Kawahara, "1.5 μm band efficient broadband wavelength conversion by difference frequency generation in a periodically domain-inverted $LiNbO_3$ channel waveguide," *Appl. Phys. Lett.*, vol. 63, no. 26, pp. 3559–3561, 1993.

[2] M. H. Chou, J. Hauden, M. A. Arbore, and M. M. Fejer, "1.5-μm-band wavelength conversion based on difference-frequency generation in $LiNbO_3$ waveguides with integrated coupling structures," *Opt. Lett.*, vol. 23, no. 13, pp. 1004–1006, 1998.

[3] J. Wang, J. Sun, C. Lou, and Q. Sun, "Experimental demonstration of wavelength conversion between ps-pulses based on cascaded sum- and difference frequency generation (SFG+DFG) in $LiNbO_3$ waveguides," *Opt. Express*, vol. 13, no. 19, pp. 7405–7414, 2005.

[4] A. S. Helmy, P. Abolghasem, J. S. Aitchison, B. J. Bijlani, J. Han, B. M. Holmes, D. Hutchings, U. Younis, and S. J. Wagner, "Recent advances in phase matching of second-order nonlinearities in monolithic semiconductor waveguides," *Laser Photonics Rev.*, 2010, to be published.

[5] A. Fiore, V. Berger, E. Rosencher, P. Bravetti, and J. Nagle, "Phase matching using an isotropic nonlinear optical material," *Nature*, vol. 391, pp. 463–466, 1998.

[6] E. Guillotel, M. Ravaro, F. Ghiglieno, C. Langlois, C. Ricolleau, S. Ducci, I. Favero, and G. Leo, "Parametric amplification in GaAs/AlOx waveguide," *Appl. Phys. Lett.*, vol. 94, no. 17, pp. 171 110–3, 2009.

[7] S. J. B. Yoo, C. Caneau, R. Bhat, M. A. Koza, A. Rajhel, and N. Antoniades, "Wavelength conversion by difference frequency generation in AlGaAs waveguides with periodic domain inversion achieved by wafer bonding," *Appl. Phys. Lett.*, vol. 68, no. 19, pp. 2609–2611, 1996.

[8] O. Levi, T. J. Pinguet, T. Skauli, L. A. Eyres, K. R. Parameswaran, J. S. Harris, Jr., M. M. Fejer, T. J. Kulp, S. E. Bisson, B. Gerard, E. Lallier, and L. Becouarn, "Difference frequency generation of 8-μm radiation in orientation-patterned GaAs," *Opt. Lett.*, vol. 27, no. 23, pp. 2091–2093, 2002.

[9] J.-B. Han, P. Abolghasem, D. Kang, B. J. Bijlani, and A. S. Helmy, "Difference-frequency generation in AlGaAs Bragg reflection waveguides," *Opt. Lett.*, vol. 35, no. 14, pp. 2334–2336, 2010.

[10] A. S. Helmy, D. C. Hutchings, T. C. Kleckner, J. H. Marsh, A. C. Bryce, J. M. Arnold, C. R. Stanley, J. S. Aitchison, C. T. A. Brown, K. Moutzouris, and M. Ebrahimzadeh, "Quasi phase matching in GaAs–AlAs superlattice waveguides through bandgap tuning by use of quantum-well intermixing," *Opt. Lett.*, vol. 25, no. 18, pp. 1370–1372, 2000.

[11] J. H. Marsh, "Quantum well intermixing," *Semi. Sci. Technol.*, vol. 6, pp. 1136–1155, 1993.

[12] U. Younis, B. M. Holmes, D. C. Hutchings, and J. S. Roberts, "Towards monolithic integration of nonlinear optical frequency conversion," *IEEE Photonics Technol. Lett.*, vol. 20, pp. 1258–1260, 2010.

[13] D. C. Hutchings, "Theory of ultrafast nonlinear refraction in semiconductor superlattices," *IEEE J. Sel. Top. Quantum Electron.*, vol. 10, no. 5, pp. 1124–1132, 2004.

[14] S. J. Wagner, B. M. Holmes, U. Younis, A. S. Helmy, J. S. Aitchison, and D. C. Hutchings, "Continuous wave second-harmonic generation using

domain-disordered quasi-phase matching waveguides," *Appl. Phys. Lett.*, vol. 94, no. 15, pp. 151 107–3, 2009.

[15] D. C. Hutchings, S. J. Wagner, B. M. Holmes, U. Younis, A. S. Helmy, and J. S. Aitchison, "Type-II quasi-phase matching in periodically intermixed semiconductor superlattice waveguides," *Opt. Lett.*, vol. 35, no. 8, pp. 1299–1301, 2010.

[16] T. C. Kleckner, A. S. Helmy, K. Zeaiter, D. C. Hutchings, and J. S. Aitchison, "Dispersion and modulation of the linear optical properties of GaAs-AlAs superlattice waveguides using quantum-well intermixing," *IEEE J. Quantum Electron.*, vol. 42, pp. 280–286, 2006.

[17] O. P. Kowalski, C. J. Hamilton, S. D. McDougall, J. H. Marsh, A. C. Bryce, R. M. De La Rue, B. Vogele, C. R. Stanley, C. C. Button, and J. S. Roberts, "A universal damage induced technique for quantum well intermixing," *Appl. Phys. Lett.*, vol. 72, no. 5, pp. 581–583, 1998.

Sean J. Wagner (S'98–M'08) obtained his B.A.Sc. degree in Computer Engineering at the University of Waterloo, Waterloo, Canada in 2003, and obtained his M.A.Sc. degree and completed his Ph.D. degree in Electrical Engineering at the University of Toronto, Toronto, Canada in 2006 and 2010, respectively.

He has previously held positions at Royal Philips Electronics, Waterloo, Canada, where he worked on semiconductor metrology systems, and at Evertz Microsystems, Burlington, Canada, where he developed fiber optic components for transmission of high-definition television signals. In his graduate research at the University of Toronto, he investigated all-optical switching and wavelength conversion devices based on semiconductor superlattices, nonlinear optics, and monolithic integration techniques. During this time, he held an NSERC Postgraduate Scholarship and he was awarded the SPIE Scholarship in Optical Science and Engineering in 2009. His research interests include semiconductor nanofabrication, nonlinear optics, photonic integrated circuits, all-optical signal processing, and optical interconnects.

Mr. Wagner is a member of the Optical Society of America and SPIE.

Barry M. Holmes graduated with the Coventry University Prize for Physics in 1996 and went on to obtain his Ph.D in 2000.

He joined Surface Technology Systems Plc. in Newport, South Wales and two years later became a Scientific Consultant. In 2003, he joined the Opto-Electronics Research Group at the University of Glasgow, where he currently holds the position of Senior Research Fellow. His research interests include integrated optical, magneto-optical and optoelectronic systems, photonic integrated circuits, non-linear optical systems and quantum cascade devices.

Usman Younis received his B.E. degree in Computer Software Engineering and his M.S. degree in Information Technology from the National University of Science and Technology, Pakistan, in 2004 and 2006, respectively, and his Ph.D. degree in Electronics and Electrical Engineering from the University of Glasgow, Glasgow, U.K. in 2010.

His research interests include III-V fabrication technologies, integrated optoelectronics, laser physics, and applied non-linear optics.

Iliya Sigal earned his B.A.Sc. degree in Engineering Science (Physics Option) and his M.A.Sc. degree in Electrical Engineering from the University of Toronto, Toronto, Canada in 2008 and 2010, respectively.

His undergraduate thesis work was done with Prof. Helmy on Raman spectroscopy of periodically intermixed AlGaAs superlattices. He also held summer research assistantships in the Physics department at the University of Toronto, working with the Nonlinear Optics and Ultracold Atoms groups. In his graduate studies, he worked on nonlinear pulse propagation in AlGaAs superlattice waveguides. His other research interests include nonlinear optics, electromagnetic pulse propagation, electro-optics, and quantum optics.

Amr S. Helmy (M'99-SM'06) received the B.Sc. degree in electronics and telecommunications engineering from Cairo University, Cairo, Egypt, in 1993, and the M.Sc. and Ph.D. degrees with a focus on photonic fabrication technologies from the University of Glasgow, Glasgow, U.K., in 1994 and 1999, respectively.

Prior to his academic career, he held a position at Agilent Technologies Photonic Devices, R&D Division, in the U.K. At Agilent, his responsibilities included developing distributed feedback lasers, monolithically integrated lasers, modulators, and amplifiers in InP-based semiconductors. He also developed high-powered submarine-class 980-nm InGaAs pump lasers. He is currently an Associate Professor in the Edward S. Rogers Sr. Department of Electrical and Computer Engineering, University of Toronto, Toronto, ON, Canada. His research interests include photonic device physics and characterization techniques, with emphasis on nonlinear optics in III-V semiconductors; applied optical spectroscopy in III-V optoelectronic devices and materials; and III-V fabrication and monolithic integration techniques.

Prof. Helmy is a member of the Optical Society of America.

J. Stewart Aitchison (M'96-SM'00) received the B.S. and Ph.D. degrees in physics from Heriot-Watt University, Edinburgh, U.K., in 1984 and 1987, respectively.

He was a post-doctoral Member of Technical Staff with Bellcore, NJ, from 1988 to 1990. He joined the Department of Electronics and Electrical Engineering at The University of Glasgow, Glasgow, Scotland, U.K., in 1990 as a Lecturer, was promoted to Senior Lecturer in 1995, and then to Professor in 1999. He joined the Department of Electrical and Computer Engineering at the University of Toronto, Toronto, ON, Canada, in 2001 where he holds the Nortel Chair in Emerging Technologies. He was Director of the Emerging Communications Technology Institute at the University of Toronto from 2004 to 2007, and is currently the interim director. He is currently the Vice Dean of Research in the Faculty of Applied Science and Engineering at the University of Toronto. He has seven patents, and more than 200 journal publications and 250 conference presentations to his credit. He is a world leader in the field of nonlinear optics, and is considered the leading researcher in the area of spatial optical solitons. His other research interests include all-optical switching and signal processing, optoelectronic integration, and optical biosensors.

Prof. Aitchison is a Fellow of the Optical Society of America, a Fellow of the Institute of Physics, London, U.K., and a Fellow of the Royal Society of Canada.

David C. Hutchings (M'98-SM'00) received the B.Sc. (with honors) and Ph.D. degrees in Physics from Heriot-Watt University, Edinburgh, U.K., in 1984 and 1988, respectively.

He has held Postdoctoral Research Positions at Heriot-Watt University and at CREOL, University of Central Florida, Orlando, FL. He joined the University of Glasgow, Glasgow, U.K., in 1992, where he currently holds a Personal Chair in Optical and Quantum Electronics in the School of Engineering. He has held Personal Research Fellowships from the Royal Society of Edinburgh/Scottish Office Education Department/Scottish Executive Enterprise and Lifelong Learning Department (1992-1995, 2003) and an Advanced Fellowship from the Engineering and Physical Sciences Research Council (1995-2000). He served as Associate Dean for Graduate Studies in the Faculty of Engineering at the University of Glasgow (2005–2010). He currently represents the IEEE Photonics Society on the Joint and International Councils on Quantum Electronics. He chaired subcommittee 09 for CLEO 2010. He is the leading authority on ultrafast nonlinear optics in the transparency range in semiconductors. His research interests also include optoelectronic integration, solitons, integrated magneto-optics, and computational electrodynamics. He has authored over 70 journal articles, and over 150 conference presentations.

Prof. Hutchings is a Fellow of the Institute of Physics, London, U.K.